Surface & Coatings Technology 206 (2011) 829–833

Contents lists available at ScienceDirect

Surface & Coatings Technology

journal homepage: www.elsevier.com/locate/surfcoat

He ion irradiation induced nanocrystallization in $Cu_{50}Zr_{45}Ti_5$ glassy alloy

Guoqiang Xie [a,*], Lin Shao [b], Dmitri V. Louzguine-Luzgin [a,c], Akihisa Inoue [a,c]

[a] Institute for Materials Research, Tohoku University, Sendai 980-8577, Japan
[b] Department of Nuclear Engineering, Texas A&M University, Texas 77843, USA
[c] WPI Advanced Institute for Materials Research, Tohoku University, Sendai 980-8577, Japan

ARTICLE INFO

Available online 8 April 2011

Keywords:
Metallic glass
Ion irradiation
Nanocrystallization
Transmission electron microscopy
Characterization

ABSTRACT

Partial nanocrystallization induced by ion irradiation can be used to improve the surface properties in metallic glasses. We investigated the crystallization behavior and the structure of the formed nanocrystalline phases in a melt-spun $Cu_{50}Zr_{45}Ti_5$ glassy alloy irradiated with 140 keV He ions to a fluence of $1.7\times10^{17}/cm^2$. Crystalline nanoparticles were precipitated by He ion irradiation. The nanocrystalline phases were identified as a mixture of the orthorhombic $Cu_{10}Zr_7$ phase, tetragonal $CuZr_2$ phase and monoclinic CuZr phase. Hardness enhancement was observed at a depth close to the projected range of the He ions, which was related to the formation of the crystalline nanoparticles.

1. Introduction

Bulk metallic glasses (BMGs) have attracted a great deal of attention and have been considered as a new class of structural materials due to their attractive physical and chemical properties such as high strength, high corrosion resistance and so on [1,2]. However, monolithic metallic glasses usually fail by the formation of highly localized shear bands under loading at room temperature, which leads to brittle fracture features and catastrophic failure of the materials [3,4]. The poor ductility limits the extensive practical applications of BMGs. In order to overcome this disadvantage, a method that nanoscale crystalline phases was introduced into the metallic glassy matrix leading to the enhanced ductility has been proposed [1,5–7].

Some glassy-nanocrystalline composites with enhanced ductility have been developed by proper alloying with the elements having zero or positive mixing enthalpy with the major component, for example, in Cu-based [8,9] and Zr-based alloys [10]. The nanocrystallites can be formed by controlling the cooling rate upon solidification or by annealing of glassy alloys. However, these approaches are limited to certain metallic glasses only. Other approaches include electron irradiation [11–15], ion irradiation [16–19], bending [20], nanoindentation [21], and so on.

Recently, Cu-based BMGs exhibiting high mechanical strength of over 2000 MPa have been developed in Cu–Zr–Ti systems [22]. It has been demonstrated that the nanocrystallization of the Cu–Zr–Ti glassy alloys was induced by ion or electron irradiation [13–15,17,18]. However, details of the mechanisms of their nucleation and formation remain unclear. Furthermore, it has been indicated that the species and structure of the induced nanocrystalline phases were sensitive to ion species, ion or electron energy, flux, irradiation temperature and so on. In the present study, we have investigated the nanocrystallization behavior of a $Cu_{50}Zr_{45}Ti_5$ metallic glassy alloy under 140 keV He ion irradiation. The structure of the nanocrystalline phases was characterized. The $Cu_{50}Zr_{45}Ti_5$ glassy alloy was selected due to its attractive mechanical properties and with well investigation on its crystallization kinetics [23].

2. Experimental procedures

Master ingots of the $Cu_{50}Zr_{45}Ti_5$ alloy (composition is given in at.%) were prepared by arc melting a mixture of high purity Cu, Zr and Ti metals in a Ti-getter high-purity argon atmosphere. The pre-alloyed ingots were re-melted at least four times in order to ensure chemical homogeneity. Ribbon samples of about 20 μm in thickness and 1.5 mm in width were prepared by rapid solidification of the melting master ingots on a single copper roller at a peripheral velocity of 42 m/s in an argon atmosphere. The thermal stability associated with the glass transition and crystallization was studied by differential scanning calorimetry (DSC) at a heating rate of 0.67 K/s.

The sample was cut into pieces and irradiated at room temperature with 140 keV He ions to a fluence of $1.7\times10^{17}/cm^2$. Beam heating is measured to be less than 50 K [17]. Microindentation tests were performed. The indentation hardness and indentation modulus of the as melt-spun ribbons and the irradiated $Cu_{50}Zr_{45}Ti_5$ samples were measured by means of an indentation load and depth sensing apparatus, a commercial Fischerscope HM2000 with a Vicker's indenter. The indentation depth for each sample was set from 300 nm to 1000 nm with increment of 100 nm and from 1300 nm 3000 nm with increment of 200 nm. A minimum of three indents for each indentation depth was performed on the samples.

* Corresponding author. Tel.: +81 22 215 2492.
E-mail address: xiegq@imr.tohoku.ac.jp (G.Q. Xie).

0257-8972/$ – see front matter © 2011 Elsevier B.V. All rights reserved.
doi:10.1016/j.surfcoat.2011.04.002

The structure of as melt-spun ribbons was examined by X-ray diffractometry (XRD) in reflection with a monochromatic Cu Kα radiation, and conventional and high-resolution transmission electron microscopy (CTEM and HRTEM). Thin foils for TEM observations were cut out from the melt-spun ribbons, followed by mechanical thinning and then by argon ion milling. In this study, a low-energy ion milling at about 2.0 kV was used to avoid the ion-beam induced crystallization. For the irradiated samples, thin foils for the TEM observation were fabricated at a depth of approximately 600 nm from the surface of the irradiated samples. The depth of 600 nm corresponds to the projected range of 140 keV He ions in the $Cu_{50}Zr_{45}Ti_5$ alloy according to the calculation using the Stopping and Range of Ions in Matter (SRIM) code [24]. TEM investigation was carried out at room temperature using a JEM-2010 (JEOL) electron microscope operating at 200 kV equipped with an X-ray energy dispersive spectrometer (EDS) of 0.1 keV resolution.

3. Results and discussion

The microstructure of as melt-spun ribbon samples before irradiation was investigated with a TEM. Fig. 1a–c show the TEM images of the melt-spun $Cu_{50}Zr_{45}Ti_5$ specimen before He ion irradiation. Fig. 1a is a bright field (BF) TEM micrograph of the specimen. No trace of crystalline phases and precipitates are found. Fig. 1b gives the corresponding selected-area diffraction (SAD) pattern. Only halo rings are observed. Fig. 1c shows a dark field (DF) TEM micrograph corresponding to Fig. 1a taken with the position “A” indicated in Fig. 1b. No crystalline phase is observed. Fig. 1d shows a typical example of an HRTEM image of the as melt-spun $Cu_{50}Zr_{45}Ti_5$ alloy ribbon. Maze-like patterns corresponding to a glassy phase are seen. Furthermore, based on the XRD and DSC analyses (not shown here), the as melt-spun $Cu_{50}Zr_{45}Ti_5$ alloy ribbon sample also showed only a glassy phase. These results indicate the absence of crystalline phase in the melt-spun $Cu_{50}Zr_{45}Ti_5$ ribbon specimens [13,15,19].

Fig. 2a shows a bright-field TEM micrograph of the sample irradiated by 140 keV He ions to a fluence of $1.7\times10^{17}/cm^2$. The bright spots in Fig. 2a correspond to helium bubbles and/or voids formed in the irradiated sample. It is difficult to distinguish one from the other since both types of defects are open volume defects [17]. Such defects are frequently observed in gas-atom irradiated alloys [25]. The half width of 140 keV He implant distribution is around 100 nm. If all implanted He atoms are retained at the end of their ranges, the He concentration near the peak region is estimated to be around 6×10^{21} atoms/cm^3 [17]. It is observed that the crystalline nanoparticles are formed, as indicated in arrows in Fig. 2a. The nanocrystallites have irregular shapes and sizes ranging from a few nanometers up to several ten nanometers. Nanocrystal formation is further confirmed by the SAD pattern (Fig. 2b) and dark-field TEM micrograph (Fig. 2c). Discontinuous Debye rings and/or sharp diffraction spots together with the broad halo rings are seen, as shown in Fig. 2b. Appearance of new electron diffraction spots in the SAD pattern of the sample upon He ion irradiation indicates that the glassy phase cannot maintain the full glassy structure and crystallization is induced by He ion irradiation. Fig. 2c is a dark-field TEM image corresponding to Fig. 2a taken with the position “A” indicated in Fig. 2b. It is seen that the crystalline nanoparticles are homogenously dispersed in the glassy matrix.

Further characterization of the crystalline nanoparticles induced by He ion irradiation was carried out using HRTEM, nano-beam electron diffraction (NBD) and EDS. Fig. 2d shows an HRTEM micrograph of the sample irradiated by 140 keV He ions to a fluence of $1.7\times10^{17}/cm^2$. Some of the nanocrystallites induced by He ion irradiation are indicated with the arrows in Fig. 2d. Fig. 3 shows some typical NBD patterns. By combining the results of the HRTEM image analyses of the crystalline nanoparticles, identifications of the NBD patterns, as well as the EDS analyses (the data have not been shown here), the formed crystalline phases are demonstrated to be a mixture consisting of an orthorhombic $Cu_{10}Zr_7$ phase (Pearson symbol: oC68), a tetragonal $CuZr_2$ phase (Pearson symbol: tI6) and a monoclinic CuZr phase (Pearson symbol: mP4) [26].

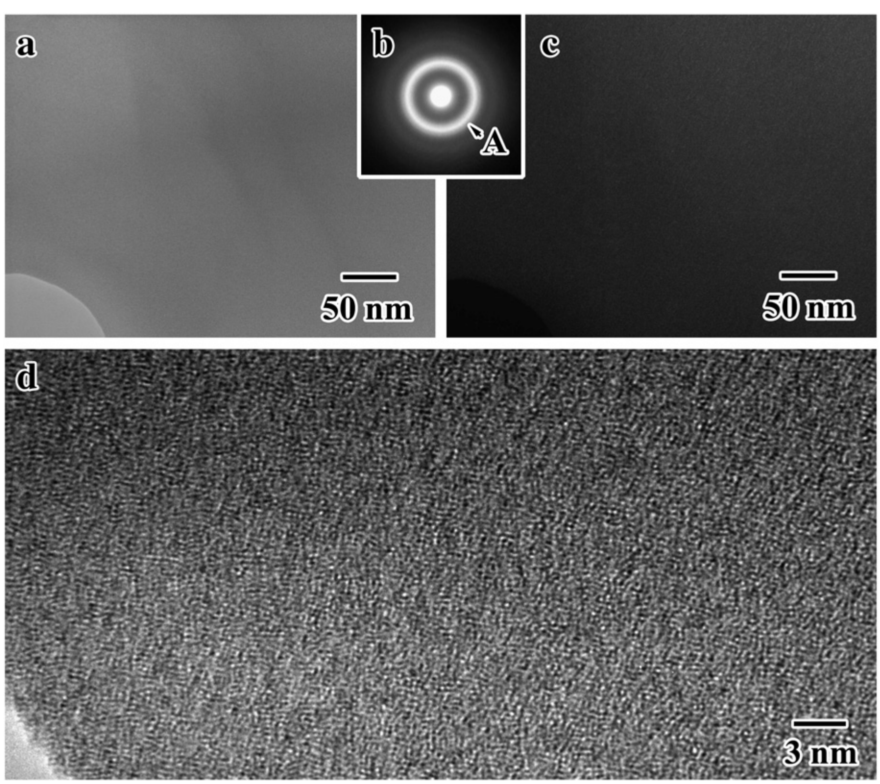

Fig. 1. TEM micrographs of as melt-spun $Cu_{50}Zr_{45}Ti_5$ ribbon sample. (a) Bright-field TEM image; (b) SAD pattern; (c) corresponding dark-field TEM image of (a) taken with the position “A” in (b) and (d) HRTEM image.